Rewrite (46),

$$\exp\left[2\Gamma_L(s_n)l\right] = \frac{A-1}{A+1} = \left(\frac{Z_L - Z_0}{Z_L + Z_0}\right)^2 \equiv R^2. \quad (47)$$

$R$, defined by (47), represents the reflection coefficient at the boundary surface $a$ or $b$. Therefore, if we set as

$$R = e^{-L_r} \quad (48)$$

then $L_r$ denotes the reflection loss at those boundary surfaces. Using the foregoing relation, (47) becomes

$$\Gamma(s_n)l = -L_r + jn\pi. \quad (49)$$

Remembering that, in the most practical cases, $\epsilon \gg |\chi(s)|$, the pole $s_n$ can be written, with the aid of (15), as

$$s_n = 2(\alpha_n l - L_r)(\delta f) + j\omega_n. \quad (50)$$

The residue for this pole $S_n$ is

$$\rho_t = \frac{(-1)^n E_0 e^{s_n t}}{|B|\,\Gamma'(s_n)l(s_n - j\omega)}. \quad (51)$$

Similarly, the residue for the pole of $F_i(s)$ in (42) is given by

$$\phi_r = E_0 Y_r(j\omega)e^{j\omega t} \quad (52)$$

and for the pole of $Y_r(s)$,

$$\rho_r = \frac{E_0 e^{s_n t}}{|B|\,\Gamma'(s_n)l(s_n - j\omega)}. \quad (53)$$

According to the Cauchy fundamental integral theorem, the closed line integral along a closed contour $ABCDA$ can now be given by the sum of all these residues enclosed. On the other hand, the contributions along a path $C_p$ vanish in the limit when $\eta_p$ approaches infinity as shown in (44). Accordingly,

$$\lim_{\eta_p \to \infty} \oint F(s)\,Y(s)e^{st}ds = \int_{\xi - j\omega}^{\xi + j\omega} F(s)\,Y(s)e^{st}ds = 2\pi j \Sigma(\phi + \rho). \quad (54)$$

Finally, substituting (45) and (51) or (52) and (53) into the foregoing equation, the transmitted and reflected electric fields can be expressed in terms of the function of time as follows:

$$E_t(t) = E_0 Y_t(j\omega)e^{j\omega t} + \sum_n (-1)^n E_n e^{s_n t} \quad (55)$$

$$E_r(t) = E_0 Y_r(j\omega)e^{j\omega t} + \sum_n E_n e^{s_n t}. \quad (56)$$

## References


[1] Jacobs, H., D. A. Holmes, L. Hatkin, and F. A. Brand, Maximum gain for forward- and backward-wave optical maser amplifiers, *J. Appl. Phys.*, vol 34, Sep 1963, pp 2617–2624.

[2] ——, D. A. Holmes, F. A. Brand, and L. Hatkin, Five layer optical maser amplification, *IEEE Trans. on Microwave Theory and Techniques*, vol MTT-12, Mar 1964, pp 163–170.

[3] Kotik, J., and M. C. Newstein, Theory of laser oscillation in Fabry-Perot resonators, *J. Appl. Phys.*, vol 32, Feb 1961, pp 178–186.

[4] Weber, E., *Linear Transient Analysis*, vol 1. New York: Wiley, 1954, pp 204–208.


# Characteristics of Loaded Rectangular Waveguides


Y. MUSHIAKE, SENIOR MEMBER, IEEE, AND T. ISHIDA



*Abstract*—**Electromagnetic fields of a rectangular waveguide with an arbitrarily loaded slab are theoretically analyzed. Eigenvalues for the transmission modes are presented in the form of universal eigenvalue charts. Electric field distributions in the loaded waveguide are obtained theoretically, and they are compared with the results of measurements. Power attenuation is also discussed, and attenuation charts that give the lowest limitation for the attenuation are shown. As an example of application the attenuation characteristics of waveguide resistance attenuators are investigated, and a new interpretation is derived for the phenomena where the curves of attenuation characteristics have sharp peak points.**



Manuscript received September 24, 1964; revised March 29, 1965.



Y. Mushiake is with the Dept. of Electrical Communications, Faculty of Engineering, Tohoku University, Sendai, Japan.

T. Ishida is with the Dept. of Electronic Engineering, Faculty of Engineering, Yamanashi University, Kofu, Japan.


## I. Introduction

THE TRANSMISSION characteristics of a rectangular waveguide loaded with a dielectric slab or resistive strip at the center of the waveguide parallel to the electric field have already been analyzed by several investigators [1]–[4]. However, the characteristics for a general case where the slab with an arbitrary admittance is loaded at a place with various distances from the side wall have not been given [5].

The purpose of this paper is to present such characteristics of the waveguides with some charts that show the dependence of the characteristics to the various parameters.

The calculations are made from Maxwell's equations and boundary conditions, and the results of the numerical computations are arranged in the form of eigenvalue charts and attenuation charts. Experimental corroborations are also made for the electric fields in the loaded waveguide and the attenuation along the direction of propagation.

As an example of application, the attenuation characteristics of waveguide resistance attenuators are investigated, and a new interpretation is derived for the phenomena where the curves of attenuation characteristics have sharp peak points.

## II. Fundamental Equations

Consider a loaded waveguide whose geometry is shown in Fig. 1, where the slab is replaced by an extremely thin sheet and the waveguide is excited at $z=0$ by an empty waveguide with $TE_{10}$ mode. Then the electromagnetic fields for the loaded waveguide can be obtained from Maxwell's equations and the boundary conditions as follows:

$$\left.\begin{aligned} E_{x1} &= j\omega\mu_0 h_y A \sin h_y y \cdot e^{-jh_z Z} \\ H_{y1} &= jh_y h_z A \sin h_y y \cdot e^{-jh_z Z} \\ H_{z1} &= h_y{}^2 A \cos h_y y \cdot e^{-jh_z Z} \\ E_{y1} &= E_{z1} = H_{x1} = 0 \end{aligned}\right\}, \quad 0 \le y < d, \tag{1}$$

$$\left.\begin{aligned} E_{x2} &= j\omega\mu_0 h_y A\zeta \sin h_y(b-y) \cdot e^{-jh_z Z} \\ H_{y2} &= jh_y h_z A\zeta \sin h_y(b-y) \cdot e^{-jh_z Z} \\ H_{z2} &= -h_y{}^2 A\zeta \cos h_y(b-y) \cdot e^{-jh_z Z} \\ E_{y2} &= E_{z2} = H_{x2} = 0 \end{aligned}\right\}, \quad d < y \le b, \tag{2}$$

$$\zeta = \sin h_y d / \sin h_y(b-d), \tag{3}$$

$$h_y{}^2 + h_z{}^2 - \omega^2\epsilon_0\mu_0 = 0, \tag{4}$$

where $h_y = \xi + j\eta$ and $h_z = \beta - j\alpha$ are propagation constants in $y$ and $z$ directions, respectively, and $A$ is an amplitude factor. In this calculation a harmonic time-dependent factor $e^{j\omega t}$ is implicitly understood, and the time-dependent quantities are expressed by their effective values. The complex eigenvalues of $h_y$ are given by the roots of a characteristic equation

$$h_y \sin h_y b = -j\omega\mu_0 a Y \sin h_y d \sin h_y(b-d) \tag{5}$$

where $Y = G + jB$ is the admittance of a load slab per unit length along the axis of the waveguide.

The electromagnetic fields will be obtained by introducing these eigenvalues into (1), (2), (3), and (4).

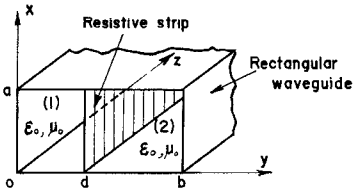


Fig. 1. Geometry of rectangular waveguide loaded with a resistive strip having an arbitrary admittance.

## III. Eigenvalues and Propagation Constants

### A. Eigenvalues of $h_y b$

From the characteristic equation (5), two sets of eigenvalues for $h_y b$ can be obtained. The one is as the roots of

$$\frac{h_y b \sin h_y b}{\sin h_y d \sin h_y(b-d)} = -j\omega\mu_0 ab Y, \tag{6}$$

when $\sin h_y d \sin h_y(b-d) \neq 0$, and the other is as

$$\left.\begin{aligned} h_y b &= \xi b = m\pi, \quad \eta b = 0, \\ h_y d &= n\pi \end{aligned}\right\}, \tag{7}$$

when these conditions are satisfied, where $m$ and $n$ are positive integers.

It is easily found that (6) has a number of roots for one value of the admittance $Y$, and the value of $h_y b$ has a number of branch points on the complex plane of $Y$. These values of $h_y b$ have been computed by digital computer. In order to show them in the form of charts for practical use, many sheets of Riemann surfaces are considered, where branch cuts are placed on the lines of $\xi b =$ constant for convenience. The values on each of these Reimann surfaces correspond to the eigenvalues for one mode, and the mode that has the smallest value of $\xi b$ in these surfaces is named as the first mode, and the one that has the second smallest value of $\xi b$ as the second mode, and so on.

A few examples of the eigenvalue charts [6] for the first two modes, where the real and the imaginary parts of the eigenvalues are plotted on the complex plane of admittance $Y$, are shown in Fig. 2.

With these charts the real and the imaginary parts of the complex eigenvalues of $h_y b$ or the values of $\xi b$ and $\eta b$ are obtainable for any given value of the load admittance $Y$ or any combination of $\omega\mu_0 abG$ and $\omega\mu_0 abB$. The relations shown with these charts hold for arbitrary values of $a$, $b$, and $\omega$. In other words, these charts may be called the universal eigenvalue charts for a loaded rectangular waveguide.

### B. Complex Propagation Constants

Multiplying (4) by $\lambda_0$, the wavelength in free space, and separating the real and the imaginary parts, one obtains universal relations as follows:

$$\alpha\lambda_0 = \frac{1}{\sqrt{2}}\left[\sqrt{\{(2\pi)^2 - (\xi\lambda_0)^2 + (\eta\lambda_0)^2\}^2 + 4(\xi\lambda_0)^2(\eta\lambda_0)^2} - \{(2\pi)^2 - (\xi\lambda_0)^2 + (\eta\lambda_0)^2\}\right]^{1/2}, \text{ (neper)}, \tag{8}$$

$$\beta\lambda_0 = \frac{1}{\sqrt{2}}\left[\sqrt{\{(2\pi)^2 - (\xi\lambda_0)^2 + (\eta\lambda_0)^2\}^2 + 4(\xi\lambda_0)^2(\eta\lambda_0)^2} + \{(2\pi)^2 - (\xi\lambda_0)^2 + (\eta\lambda_0)^2\}\right]^{1/2}, \text{ (rad.)}. \tag{9}$$

These values of $\alpha\lambda_0$ and $\beta\lambda_0$ are plotted in Figs. 3 and 4 vs. $\xi\lambda_0$ for various values of the parameter $\eta\lambda_0$. By making use of Fig. 2 or (7) and Figs. 3 and 4, the phase constants and the attenuation constants for an arbitrarily loaded rectangular waveguide of any size will be determined easily.

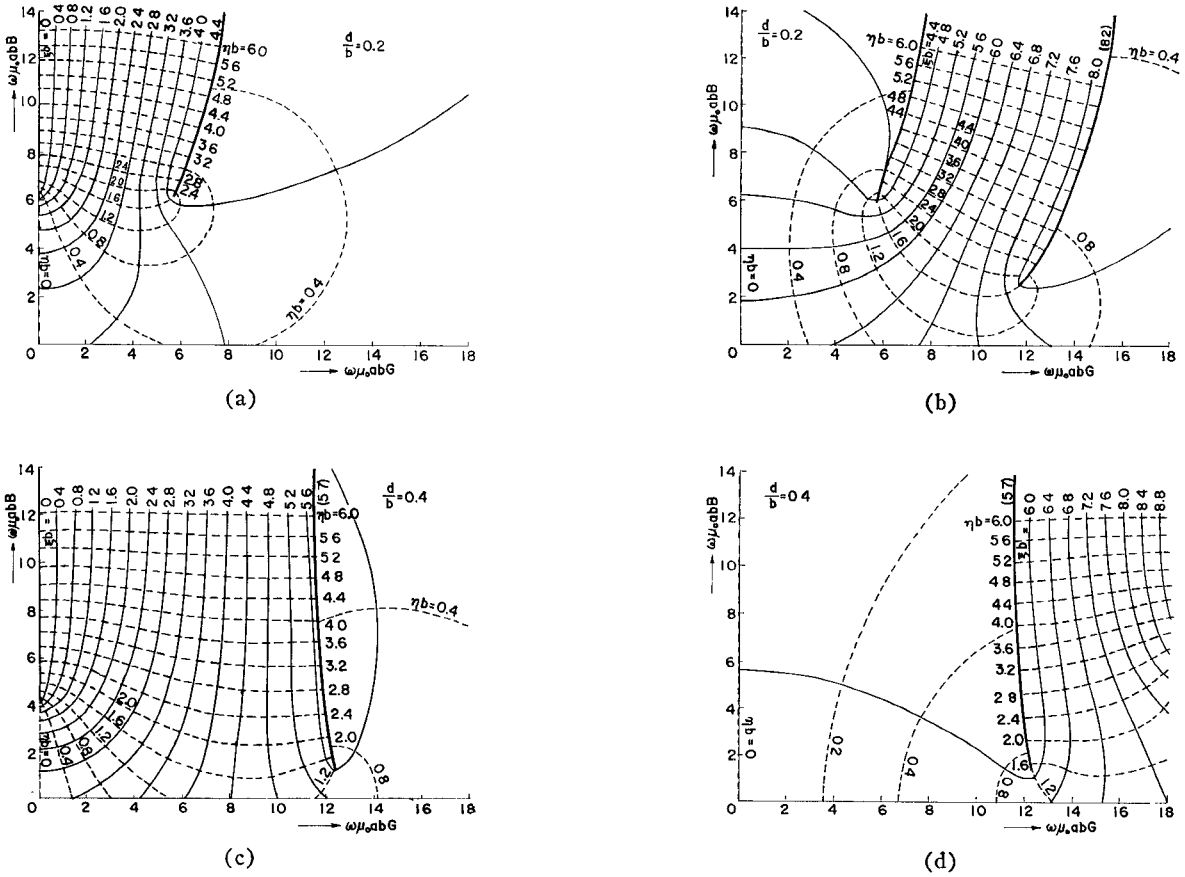


Fig. 2. Eigenvalue charts. (a) $d/b=0.2$, the first mode. (b) $d/b=0.2$, the second mode. (c) $d/b=0.4$, the first mode. (d) $d/b=0.4$, the second mode.

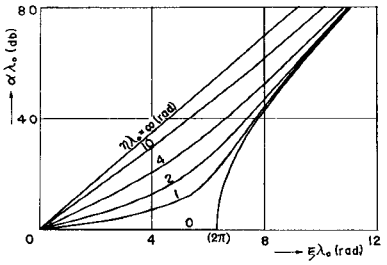

Fig. 3. Universal curves for the normalized attenuation constant $\alpha\lambda_0$ plotted vs. $\xi\lambda_0$ with parameter $\eta\lambda_0$.

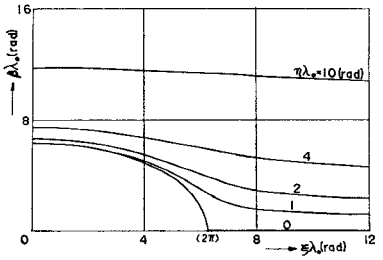

Fig. 4. Universal curves for the normalized phase constant $\beta\lambda_0$ plotted vs. $\xi\lambda_0$ with parameter $\eta\lambda_0$.

## IV. Electromagnetic Fields in the Loaded Waveguide

For simplicity it is assumed here that the effect of the load admittance is so small that the shape of the electric field distribution at the excitation surface $z=0$ is nearly equal to that of $TE_{10}$ in the empty waveguide. In this case the amplitude factor $A_m$ for $m$th mode can be determined by taking into account the orthogonality [7] for the electric fields of the loaded waveguide modes as follows:

$$\frac{A_m}{A_0}=\frac{\pi}{\pi+h_{ym}b}\left[\sin\left(\pi\frac{d}{b}+h_{ym}d\right)+\zeta_m\sin\left\{\pi\frac{d}{b}-h_{ym}(b-d)\right\}\right]\cdot\frac{1}{\Delta_m}$$

$$-\frac{\pi}{\pi-h_{ym}b}\left[\sin\left(\pi\frac{d}{b}-h_{ym}d\right)+\zeta_m\sin\left\{\pi\frac{d}{b}+h_{ym}(b-d)\right\}\right]\cdot\frac{1}{\Delta_m},\qquad(10)$$

where

$$\Delta_m=\tfrac{1}{2}\{\sin 2h_{ym}d+\zeta_m^2\sin 2h_{ym}(b-d)\}-\{h_{ym}d+\zeta_m^2h_{ym}(b-d)\},\qquad(11)$$

and $A_0$ is the amplitude factor of $TE_{10}$ in the empty waveguide.

From (10) it is easily found that $(h_{ym}/h_{y0})(A_m/A_0)\propto 1/m^2$ for $m\gg 1$, and the value of amplitude factor $A_m$ for higher mode diminishes very rapidly with increasing

$m$, the order of higher mode. For this reason, it is sufficient in this case to take only the first several modes for the approximate expressions of the electromagnetic fields in the loaded waveguide.

## V. Numerical Example of the Electric Fields

### A. Admittance of the Load Slab

Throughout the theory just described the thickness of the load slab is neglected, but the actual load always has a finite thickness, and the theory cannot be applied directly to such a case. When the thickness is considerably small compared with the width of waveguide, however, it is found from the experiments that the effects of the thickness are negligible if an equivalent admittance of the load slab is introduced in place of the sheet admittance [8]. For example, an equivalent admittance of dielectric plate loaded in the waveguide is given by

$$B_0 = (1/a)\omega\epsilon_0(\kappa_e - 1)t \tag{12}$$

where $\kappa_e$ is specific dielectric constant, $t$ is the thickness, and $a$ is the height of the waveguide. In the case of attenuators, however, such a dielectric base plate is coated with a conducting thin film of metal or carbon, which has resistive or capacitive impedance in general [9].

### B. Computation of the Electric Fields

Numerical computations have been made of the electric fields in the loaded waveguide with the method just described by taking only the first two modes. The dimensions of the waveguide and the construction of the

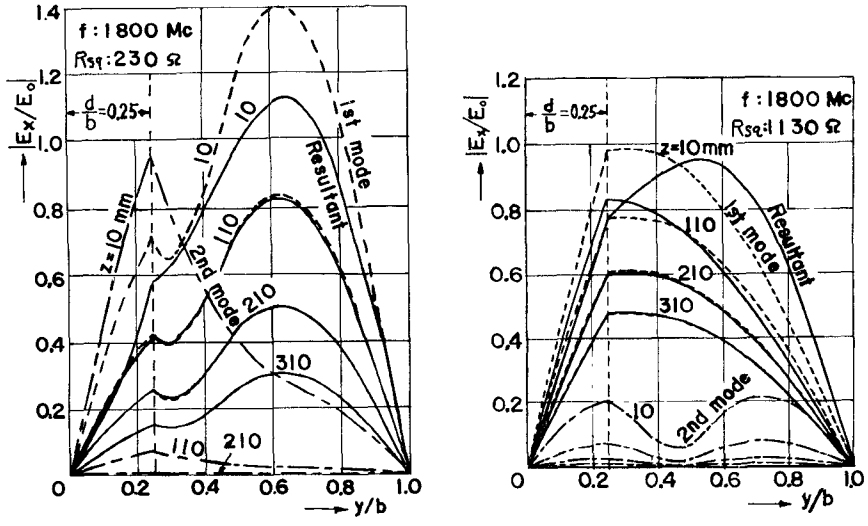


Fig. 5. The first mode, the second mode, and the resultant electric field patterns. (a) $R_{sq}=230\ \Omega$, $f=1800$ Mc, $d/b=0.25$. (b) $R_{sq}=1130\ \Omega$, $f=1800$ Mc, $d/b=0.25$.

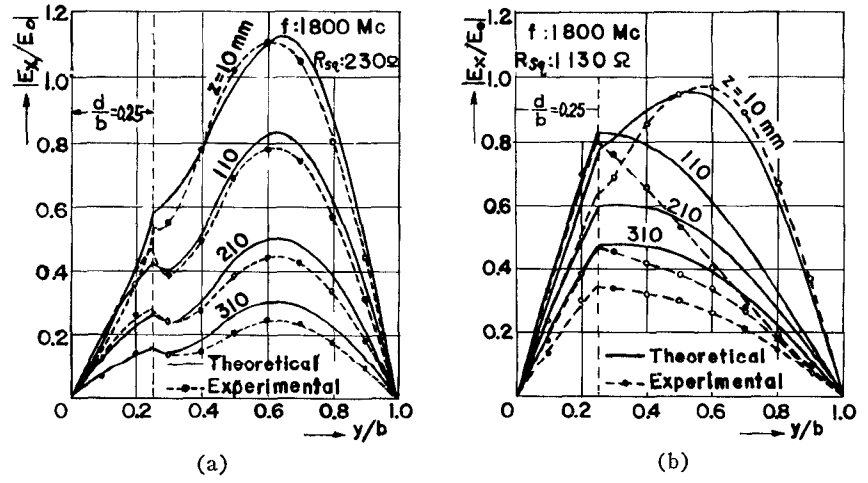


Fig. 6. Examples of measured electric field patterns. (a) $R_{sq}=230\ \Omega$ $f=1800$ Mc, $d/b=0.25$. (b) $R_{sq}=1130\ \Omega$, $f=1800$ Mc, $d/b=0.25$.

load are as follows:

$a = 75$ mm, $b = 150$ mm,
$d/b = 0.1$, 0.25, and 0.4, $f = 1800$ Mc,

thickness of the base plate (bakelite) = 4 mm, surface resistance of resistive film (carbon film), $R_{sq} = 230\ \Omega$ and $1130\Omega$, hence,

$$Y = 57.7 + j37.0 \text{ (millimho/m)}$$

and

$$11.8 + j20.2 \text{ (millimho/m)}.$$

Examples of the distribution of $E_x$ for the first and the second modes and the resultant fields at various values of $z$ are shown in Fig. 5. Measurements of the total electric fields for various values of $z$ have also been made under the same conditions, and the measured values are compared with theoretical ones in Fig. 6, which shows fairly good agreements between them.

## VI. Attenuation in the Loaded Waveguide

### A. General Consideration

For the loaded waveguides with lossy admittances the orthogonality relations for the powers between two modes do not exist [10], and the transmission power $P_l$ at $z = l$ is generally given by

$$P_l = \sum_{m=1}^{\infty} \sum_{n=1}^{\infty} \text{Re}\,(P_{cmn}) \tag{13}$$

where $P_{cmn}$ is the complex power between the electric field of $m$th mode and the magnetic field of $n$th mode defined by

$$P_{cmn} = \int_S E_{xm} H_{yn}^* dS. \tag{14}$$

It should be noted here that the mutual power $P_{cmn}$ is not equal to $P_{cnm}$ in general. However, a relation between $P_{cmn}$ and $P_{cnm}$ can be derived from (1) and (14), that is,

$$[P_{cmn} h_{zm}]^* = P_{cnm} h_{zn}. \tag{15}$$

As for the attenuation of the transmission power, there exists a general expression

$$\gamma = 10 \log_{10} (P_0/P_l) \tag{16}$$

where $\gamma$ is the power attenuation for the loaded waveguide with the length $l$.

### B. Approximation in the Calculation of Attenuation

From the analysis described in the preceding sections it is easily found that the attenuation constants of the higher modes of the loaded waveguide are extremely large compared with that of the first or the second mode. Moreover, the amplitude factors for the higher modes are usually very small as mentioned in Section IV. For these two reasons, it will be sufficient to take only a few terms of (13) in the computation of the transmission power $P$ at the point where the distance from the excitation point is not too small.

According to several examples of numerical computation for the loaded waveguides with the dimensions of $b < \lambda_0$ and $a < \lambda_0/2$, the attenuation constants for the third and the higher modes are always very large, but sometimes the attenuation constant of the second mode becomes smaller than that of the first mode if the value of $d/b$ is not near zero and the load admittance is not too small.

By taking these facts into consideration, the following approximate expression is employed in the computation:

$$P_l \simeq P_{11} + P_{12} + P_{21} + P_{22}, \tag{17}$$

where $P_{mn}$ is the real part of the complex power $P_{cmn}$. Figure 7 shows two examples of the attenuations computed from (17) and plotted vs. $d/b$ for fixed value of the load admittance. The attenuations of the first and the second modes are also shown with dashed lines in the same figure.

### C. Attenuation Charts [11]

From Fig. 7 it is found that further approximation will be done for the attenuation, where the result of approximation is quite simple but still gives very important information about the characteristics of the attenuation. That is to take only one mode that has lowest attenuation in the computation of the power attenuation for the loaded waveguide. The results that will be obtained by this procedure are considered to give the lowest limitation for the attenuation. In other words, they give correct attenuation characteristics for the limiting case of infinitely long loaded waveguide. Figure 8 shows the value of attenuation per free space wavelength for such limiting case.

## VII. Application to Waveguide Attenuators

As an example of application of the present treatment let us investigate the behavior of the attenuation characteristics of a vane-type waveguide attenuator. In the practical attenuator the load plate does not contact directly with the upper and lower walls of the waveguide, but there exist small air gaps at both ends of the plate. The effects of the gaps have been studied, and a modified equivalent admittance, where the effects of slab thickness are also considered, has been introduced [12]. By taking this modified equivalent admittance and using Fig. 8, attenuation characteristics for the limiting case are determined, and the results are shown in Fig. 9. As the characteristics of variable attenuators, the curves that have irregular variations for the distance $d$ are not adequate, whereas the curves that have even variation over wide ranges of the values of attenuation and $d$ are desirable. From this point of

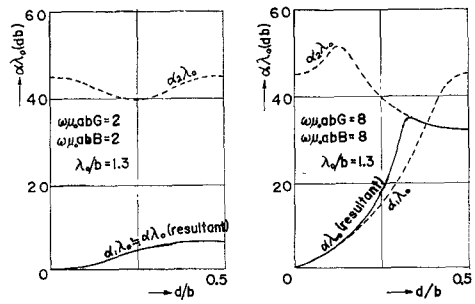


Fig. 7. Examples of theoretical attenuation constants of resistive attenuator. (a) $\omega\mu_0 abG = \omega\mu_0 abB = 2$. (b) $\omega\mu_0 abG = \omega\mu_0 abB = 8$.

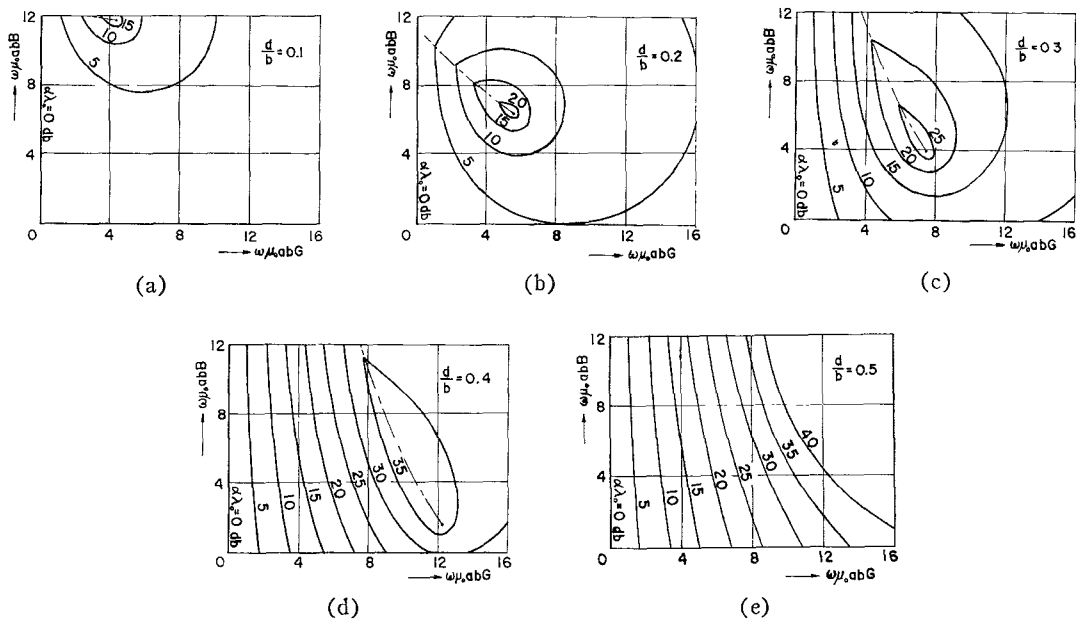


Fig. 8. Attenuation charts. (a) $d/b = 0.1$, $\lambda_0/b = 1.3$. (b) $d/b = 0.2$, $\lambda_0/b = 1.3$. (c) $d/b = 0.3$, $\lambda_0/b = 1.3$. (d) $d/b = 0.4$, $\lambda_0/b = 1.3$. (e) $d/b = 0.5$, $\lambda_0/b = 1.3$.

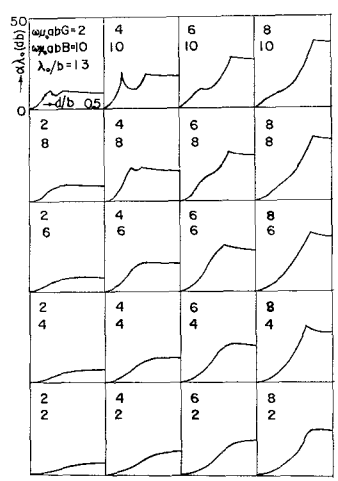


Fig. 9. Variations of attenuation characteristics for various equivalent admittances $Y = G + jB$ of resistive strips for $\lambda_0/b = 1.3$.

view Fig. 9 contains very important information about the relations between the shape of the attenuation curves and the values of normalized admittances, and it will be utilized in designing vane-type waveguide attenuators.

From Fig. 9 an interesting and entirely new interpretation about the irregular characteristics of waveguide resistance attenuators will be derived. Heretofore, the irregular variation of attenuation characteristics where some peak points exist at some distances of $d$ has been explained as a resonance phenomenon in the circuit of the load slab and the gap capacitance (e.g. [13]). However, the load slab always has capacitive reactance as understood from the considerations in Section V-A, and the resonance with the gap capacitance cannot exist. A new interpretation for such phenomena derived here is that the peak attenuation occurs around the point where the lowest attenuation mode changes from one mode to another. Such phenomena are seen in Fig. 7(b) and the curves for large admittances in Fig. 9.

## VIII. Conclusions

The electromagnetic fields of a loaded rectangular waveguide have been analyzed, and the results of the numerical computation have been presented by various curves and universal charts. Some experimental corroborations have also been made, and good agreements between the theory and the experiments have been found. Application of this study to the vane-type attenuators is discussed, and a new interpretation for the peaks in the curves of their attenuation characteristics is shown.

Although some approximations are involved in the treatment just described, it is believed that the results give valuable and new information about the characteristics of the loaded rectangular waveguides.

## Acknowledgment

The authors wish to express their sincere gratitude to Professors S. Uda and T. Oshiyama for their advice and encouragement.

## References

[1] Marcuvitz, N., *Waveguide Handbook*. New York: McGraw-Hill, 1951, pp 388–391.
[2] Berk, A. D., Variational principles for electromagnetic resonators and waveguides, *IRE Trans. on Antennas and Propagation*, vol AP-4, Apr 1956, pp 104–111.
[3] Button, K. J., and B. Lax, Theory of ferrites in rectangular waveguides, *IRE Trans. on Antennas and Propagation*, vol AP-4, Jul 1956, pp 531–537.
[4] Vartanian, P. H., W. P. Ayres, and A. L. Helgesson, Propagation in dielectric slab loaded rectangular waveguide, *IRE Trans. on Microwave Theory and Techniques*, vol MTT-6, Apr 1958, pp 215–222.
[5] Knudsen, H. L., Champ dans un guide rectangulaire a membrane conductrice, *L'onde Electrique*, no. 313, vol 33, Apr 1953, pp 217–234.
[6] Ishida, T., and Y. Mushiake, Eigenvalues for the rectangular waveguide loaded with a slab having an arbitrary admittance, *J. Inst. Elect. Commun. Engrs. (Japan)*, vol 44, Jan 1961, pp 36–41 (in Japanese).
[7] Slater, J. C., Microwave electronics, *Rev. Mod. Phys.*, vol 18, Oct 1946, pp 441–512.
[8] Ishida, T., and Y. Mushiake, Universal solution of rectangular waveguide loaded with a dielectric slab, *J. Inst. Elect. Commun. Engrs. (Japan)*, vol 43, Sep 1960, pp 943–947 (in Japanese).
[9] Ishida, T., Resistive strips for waveguide attenuators, *Rept. Fac Eng., Yamanashi Univ.*, no. 12, Dec 1961, pp 148–155 (in Japanese).
[10] Adler, R. B., Waves on inhomogeneous cylindrical structures, *Proc. IRE*, vol 40, Mar 1952, pp 339–348.
[11] Ishida, T., and Y. Mushiake, Attenuation characteristics of waveguide resistance attenuators, *J. Inst. Elect. Commun. Engrs. (Japan)*, vol 45, Oct 1962, pp 1370–1376 (in Japanese).
[12] Ishida, T., and J. Osada, Effects of gaps placed between slab and the top and bottom walls of guide in the waveguide attenuators, *Rept. Fac. Eng., Yamanashi Univ.*, no. 12, Dec 1961, pp 135–147 (in Japanese).
[13] Montgomery, C. G., *Technique of Microwave Measurements*. New York: McGraw-Hill, 1947, pp 790–799.